Chemical Form and Distribution of Selenium and Sulfur in the Selenium Hyperaccumulator *Astragalus bisulcatus*[1]

Ingrid J. Pickering, Carrie Wright, Ben Bubner, Danielle Ellis, Michael W. Persans, Eileen Y. Yu, Graham N. George, Roger C. Prince, and David E. Salt*

Department of Horticulture and Landscape Architecture, Purdue University, West Lafayette, Indiana 47907 (D.E.S., D.E.); Northern Arizona University, Flagstaff, Arizona 86011 (C.W., B.B.); Department of Biology, University of Texas-Pan American, Edinburg, Texas 78539 (M.W.P.); Stanford Synchrotron Radiation Laboratory, Stanford University, Stanford Linear Accelerator Center, Menlo Park, California 94025 (I.J.P., E.Y.Y., G.N.G.); and ExxonMobil Research and Engineering Company, Annandale, New Jersey 08801 (R.C.P.).

In its natural habitat, *Astragalus bisulcatus* can accumulate up to 0.65% (w/w) selenium (Se) in its shoot dry weight. X-ray absorption spectroscopy has been used to examine the selenium biochemistry of *A. bisulcatus*. High concentrations of the nonprotein amino acid Se-methylseleno-cysteine (Cys) are present in young leaves of *A. bisulcatus*, but in more mature leaves, the Se-methylseleno-Cys concentration is lower, and selenate predominates. Seleno-Cys methyltransferase is the enzyme responsible for the biosynthesis of Se-methylseleno-Cys from seleno-Cys and *S*-methyl-methionine. Seleno-Cys methyltransferase is found to be expressed in *A. bisulcatus* leaves of all ages, and thus the biosynthesis of Se-methylseleno-Cys in older leaves is limited earlier in the metabolic pathway, probably by an inability to chemically reduce selenate. A comparative study of sulfur (S) and Se in *A. bisulcatus* using x-ray absorption spectroscopy indicates similar trends for oxidized and reduced Se and S species, but also indicates that the proportions of these differ significantly. These results also indicate that sulfate and selenate reduction are developmentally correlated, and they suggest important differences between S and Se biochemistries.

Many selenium (Se) compounds are toxic to mammals at high concentrations, but Se is also an essential micronutrient, and low doses have been implicated in cancer prevention (Clark et al., 1996; Combs et al., 1997). Not all diets provide adequate Se, and an obvious and inexpensive way to provide Se may be to engineer food plants to accumulate higher levels of the element (Ip et al., 1994). The Se hyperaccumulator *Astragalus* species, such as *Astragalus bisulcatus*, may be an excellent source of genetic material from which to isolate genes to develop such plants. In the wild, *A. bisulcatus* can accumulate Se levels of up to 0.65% (w/w) dry weight in the shoots (Byers, 1936), predominantly as Se-methylseleno-Cys (Trelease et al., 1960), and similar results are readily obtained in plants grown hydroponically in the laboratory (Orser et al., 1999). Understanding Se uptake in *A. bisulcatus* might also allow the development of highly effective cultivars for phytoremediation (Salt et al., 1998).

A critical step in the biotransformation of selenate is the initial two-electron reduction to selenite. Hyperaccumulating plants might achieve this in at least three different ways: by substituting selenate into the sulfate reduction pathway (reduction by ATP sulfurylase/adenyl sulfate (APS) reductase; Shrift, 1969; Setya et al., 1996), by substituting selenate into the nitrate uptake pathway (microbial nitrate reductases can reduce selenate; Sabaty et al., 2001), or by a specific selenate reductase. For nonhyperaccumulating plants, there is good evidence that selenate reduction occurs via substitution for sulfate in the ATP sulfurylase/APS reductase system, and that this is the rate-limiting step in selenate transformation (Shrift, 1969; Shaw and Anderson, 1974; Burnell, 1981; Pilon-Smits et al., 1999). In these species, the biochemistries of S and Se appear to be closely linked, and the plants metabolize selenate to the Se isologs of the primary end products of the sulfate assimilation pathway: Cys, Met, and various intermediates. There is good bio-

[1] This research was supported by the U.S. National Cancer Institute (grant to D.E.S.) and by the U.S. National Institutes of Health (grants to E.Y.Y., I.J.P., and G.N.G.). During the period of this research, C.W. and D.E. were working in the laboratory of D.E.S. as employees of NuCycle Therapy (Monmouth Junction, NJ), which was supported by the U.S. National Cancer Institute (Small Business Technology Transfer grant). Portions of this research were carried out at the Stanford Synchrotron Radiation Laboratory (SSRL), a national user facility operated by Stanford University on behalf of the U.S. Department of Energy, Office of Basic Energy Sciences. The SSRL Structural Molecular Biology Program is supported by the Department of Energy, Office of Biological and Environmental Research, and by the National Institutes of Health, National Center for Research Resources, Biomedical Technology Program. The sulfur K-edge x-ray absorption spectroscopy studies at SSRL were supported by the U.S. National Institutes of Health (grant no. GM57375).

* Corresponding author; e-mail dsalt@purdue.edu; fax 765–494–0391.

Article, publication date, and citation information can be found at www.plantphysiol.org/cgi/doi/10.1104/pp.014787.

chemical and physiological evidence that selenate is taken up from the soil solution via the same root processes as sulfate (Mikkelsen and Wan, 1990; Williams et al., 1994; Barak and Goldman, 1997).

The biochemistry of Se-hyperaccumulating *A. bisulcatus* has also been studied (for review, see Shrift, 1969; Brown and Shrift, 1982), although many details remain to be clarified. If the same pathways as S are followed, the first stage would be the activation of selenate by ATP sulfurylase to form 5′-adenylylselenate (APSe; Shaw and Anderson, 1972, 1974). This enzymatic step is also required for selenate reduction in *Escherichia coli* (Muller et al., 1997). There is evidence that APSe can be nonenzymatically reduced by glutathione (Dilworth and Bandurski, 1977), but enzymatic reduction is essential in *E. coli* (Muller et al., 1997), suggesting that the nonenzymatic reduction of APSe may not occur to any significant extent in planta. Reduction of selenite to selenide appears to occur nonenzymatically in plants (Ng and Anderson, 1978) and in *E. coli* (Muller et al., 1997), which may explain why selenite is more readily assimilated by plants to organic forms than is selenate (Shrift and Virupaksha, 1965; de Souza et al., 1998).

Once present, selenide can be incorporated into seleno-Cys by the action of *O*-acetyl-Ser thiol lyase (Ng and Anderson, 1978). In Se nonaccumulator *Astragalus* species, seleno-Cys enters the Met biosynthetic pathway through the action of cystathionine-γ-synthase (McCluskey et al., 1986) to ultimately form seleno-Met and Se-methylseleno-Met (Virupaksha and Shrift, 1965). These seem to be toxic to the plants. However, in Se hyperaccumulator *Astragalus* species, seleno-Cys is methylated by seleno-Cys methyl transferase (Neuhierl and Böck, 1996; Neuhierl et al., 1999) to form Se-methylseleno-Cys in a metabolic step that is unique to these species (Wang et al., 1999), and high concentrations of this compound are tolerated by the plant.

Thus, the two-electron reduction of selenate to selenite is a major limitation that must be overcome if plants are to be engineered for accumulation of chemopreventive Se compounds (Orser et al., 1999) or for remediation of Se-contaminated soils and waters (Pilon-Smits et al., 1999). Furthermore, the capability to biosynthesize Se-methylseleno-Cys must be engineered to prevent the toxic effects of seleno-Met and to provide anticarcinogenic properties. *Astragalus* hyperaccumulator species, including *A. bisulcatus*, are good sources of genetic material for engineering enhanced Se accumulation, and a better understanding of the physiology and biochemistry of Se assimilation in *A. bisulcatus* will help to target the most critical genes involved in the process. In this study, we have used x-ray absorption spectroscopy to investigate the chemical forms of Se and S in various *A. bisulcatus* tissues.

RESULTS

Se Speciation in *A. bisulcatus* Tissues

In our previous work (Pickering et al., 2000), we used *A. bisulcatus* plants that were first grown to maturity in the absence of Se, and then had selenate gradually introduced into the hydroponic growth medium. Because this generated ambiguity about whether observed changes were due to inducible pathways or a developmental dependence (Pickering et al., 2000), the current work used plants that were grown on selenate-containing medium throughout the entire hydroponic culture. Se K near-edge x-ray absorption spectra of *A. bisulcatus* tissues at different developmental ages (Fig. 1) show large variation in the species present (Fig. 2). The spectra of the more mature tissues are dominated by the higher energy peak, corresponding to selenate (Fig. 2A), whereas the spectra of the younger tissues show predominantly lower energy features that correspond to organic Se. We modeled this species using the spectrum of seleno-Met, but in the tissues, the organic form is most likely Se-methyl seleno-Cys (Trelease et al., 1960), which has a nearly identical near-edge spectrum to seleno-Met (because the immediate local environment of Se is identical). Fitting the tissue x-ray absorption spectra to spectra of selected standard compounds, together with estimation of total

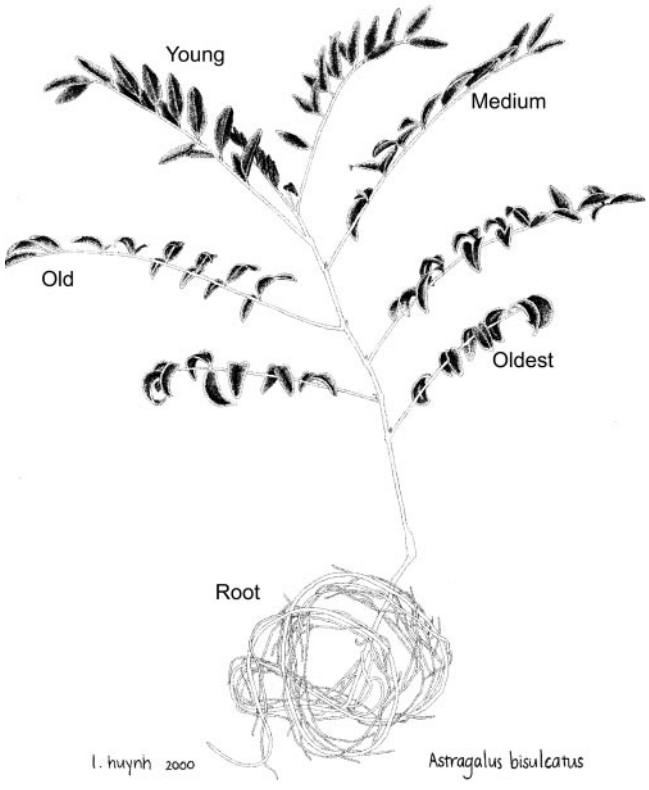

Figure 1. *A. bisulcatus* showing morphology and origin of different tissues. For the S spectroscopy only, additional tissue samples were taken from the newest leaves (called "younger" and "youngest").

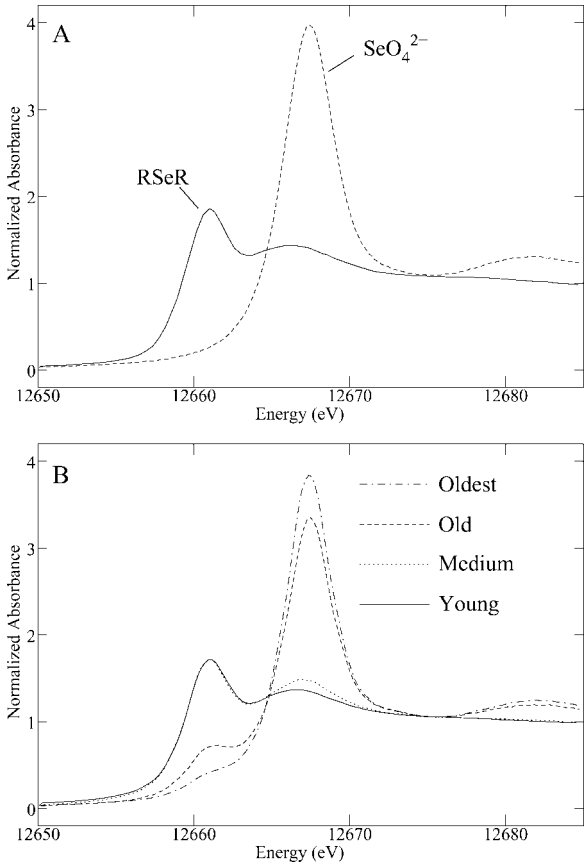

Figure 2. Se K near-edge x-ray absorption spectra of Se standards (A) and different *A. bisulcatus* tissues (B). All spectra have been normalized. The standards are aqueous seleno-Met (RSeR) and aqueous selenate (SeO_4^{2-}).

Se, allowed the quantitative estimation of the relative content of Se chemical forms in the different *A. bisulcatus* tissues (Fig. 3). The highest concentration of selenate is observed in the oldest leaves, in which it comprises 91% (w/w) of the total Se. Less mature tissues show progressively less selenate and more organic Se (Fig. 3). The greatest total Se is found in the young tissues, where 99% (w/w) is in the organic form. The young leaves show more than a 60-fold increase in organic Se, and a 15-fold decrease in selenate, relative to the oldest leaves. The roots show the lowest levels of total Se of any tissues, and their Se is 92% organic; the concentration of root organic Se appears intermediate between that of the old and intermediate tissues.

S Speciation in *A. bisulcatus* Tissues

S K near-edge x-ray absorption spectra of *A. bisulcatus* tissues at different developmental ages (Fig. 1) are shown in Figure 4B in comparison with relevant standard spectra (Fig. 4A). Similar to the Se spectra (Fig. 2), the S spectra show a partitioning between oxidized forms (mainly sulfate, indicated by the peak at around 2,480 eV), and organic forms, with peaks at around 2,471 eV. However, as predicted from the much longer core-hole lifetime, the S spectra are considerably sharper than their Se counterparts (Pickering et al., 1999), and thus, more detail can be observed. There is a shoulder on the low energy side of the sulfate peak, at around 2,478 eV (characteristic of a substituted sulfate species), which we have fitted using a methyl sulfate $[CH_3\text{-}OSO_3]^-$ standard (Fig. 4A). This species may in fact be APS $[RO\text{-}PO_2\text{-}OSO_3]^-$, an intermediate in sulfate reduction, or possibly glucosinolates (Yu et al., 2001) $[R = N - OSO_3]^-$, which are involved in a large number of plant cellular processes (Petersen et al., 2002). The reduced organic peak also shows considerable variation (Fig. 4B, inset), which results from differing proportions of reduced S species, interpreted as thiols, disulfides, and thioethers (Pickering et al., 1998).

The quantitative estimation of the relative content of S species in the different tissues of *A. bisulcatus* is shown in Figure 5. High levels of S were detected in all samples, except for the roots, which showed no detectable S at all. As with Se (see above), sulfate shows the highest concentration in the oldest tissues, with a steady progression to lower concentrations for younger tissues, and the organic S shows the reverse. However, in contrast to the Se, sulfate is the predominant form at all developmental stages except for the younger and youngest leaves; even in the young leaves, it accounts for some 62% (w/w) of the total S budget. In the younger and youngest leaves, the trends appear to continue such that the youngest leaves have the least sulfate, albeit at least 17% (w/w) compared with 1% (w/w) for selenate in the young leaf tissue. Again, in contrast to Se, the greatest total S level is found in the oldest tissues, where it is 80% (w/v) sulfate. Furthermore, the change in amounts of sulfate and organic S as a function of maturity are much less substantial than the Se case;

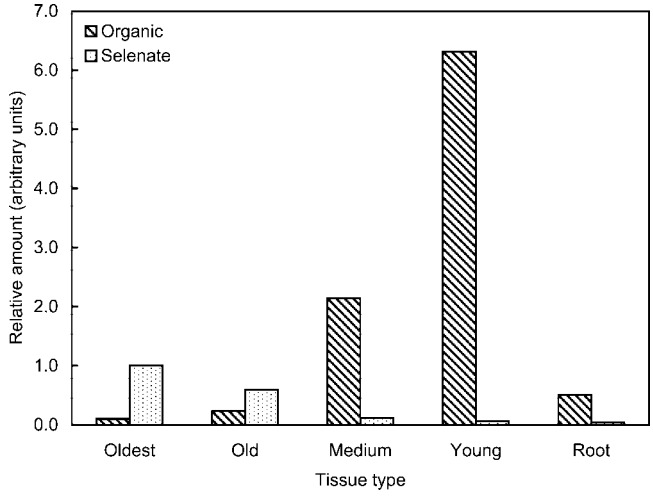

Figure 3. Relative amounts of Se species in *A. bisulcatus* tissues. The amounts are arbitrarily normalized to the selenate concentration in the oldest leaf sample.

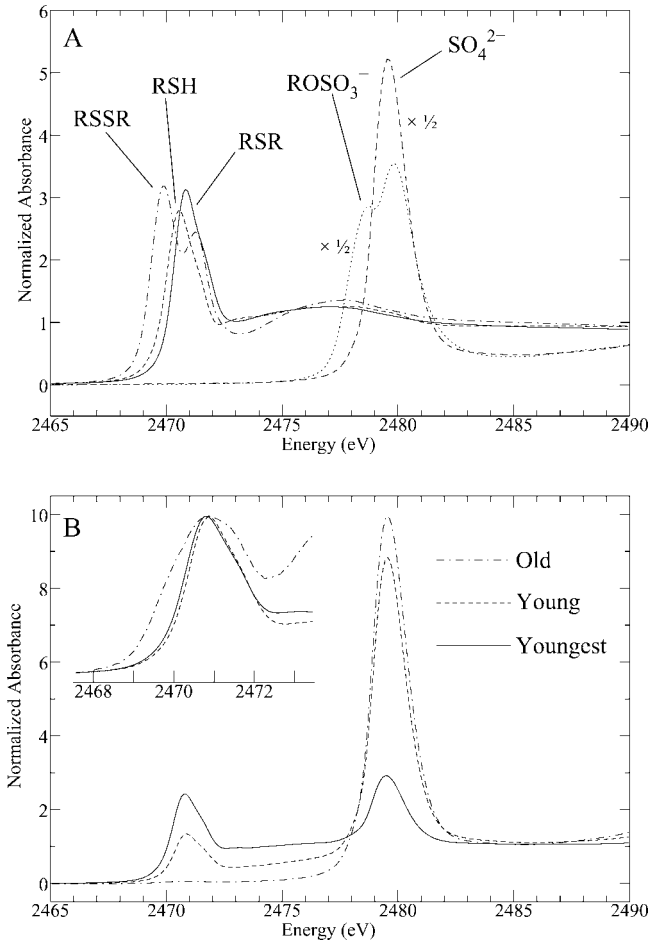

Figure 4. S K near-edge x-ray absorption spectra of S standards (A) and selected *A. bisulcatus* tissues (B). All spectra have been normalized. Spectra are displayed for the top surface of the leaves, but the bottom surface gave very similar results. The inset in B shows the reduced S region, with the spectra arbitrarily normalized to the peak intensity for clarity. The standards (all aqueous solutions) are oxidized glutathione, reduced glutathione, Met, methyl sulfate, and sulfate. The latter two have been scaled by 50%.

comparing youngest leaves with the oldest, a 10-fold decrease in sulfate and an 8-fold increase in organic are observed. The component modeled as methyl sulfate is seen to contribute some 15% (w/w) to the total S for the oldest leaves, but contributes 2% (w/w) or less to the young tissues.

Organic S species are modeled as thioether, thiol, and disulfide. Within the organic S species, there is a considerably greater fraction of disulfides present in the most mature tissues (Figs. 4B, inset and Fig. 5, inset). This might be consistent with the postulated increasingly oxidative intracellular environment as cellular development progresses (Schafer and Buettner, 2001). However, in these tissues, the total amount of organic species is not high. The thioether species dominate the organic S (>90%, w/v) for medium, young, and younger leaves, but for the youngest, some 17% (w/v) thiol contributes (resulting in a small but significant peak shift; Fig. 4B, inset).

Seleno-Cys Methyltransferase (*SMT1*) Gene and Protein Expression

SMT1 was amplified from *A. bisulcatus* total RNA by reverse transcriptase (RT)-PCR, and was directionally cloned into pZErO-2. The *SMT1* cDNA was sequenced and its identity was confirmed by alignment with the SMT1 amino acid sequence in GenBank (accession no. AJ131433). Analyses of the steady-state mRNA and protein levels of SMT revealed significant levels of expression at all developmental stages examined (Fig. 6). Expression of *SMT1* mRNA and protein in the shoots and the roots was observed in selenate-exposed and -unexposed control plants (Fig. 7). As reported by Neuhierl et al. (1999), we also observed two isoforms of the SMT1 protein in shoot tissue (Figs. 6 and 7), and a higher M_r cross-reacted protein that appears most abundant in root tissue.

DISCUSSION

We have used Se and S K-edge x-ray absorption spectroscopy to show that the developmental dependency of the S and Se metabolome of *A. bisulcatus* are similar in some respects, but different in others. In essence, the trends for oxidized and reduced Se and S species are similar, but the proportions differ quite significantly, suggesting important differences between S and Se biochemistry. At present, there is no direct evidence pertaining to whether selenate reduction in *A. bisulcatus* occurs via the ATP sulfurylase/APS reductase pathway, or via some Se-specific selenate reductase. Seleno-Cys methyltransferase appears to be expressed constitutively in *A. bisulcatus*, regardless of selenate exposure or tissue age (Figs. 6

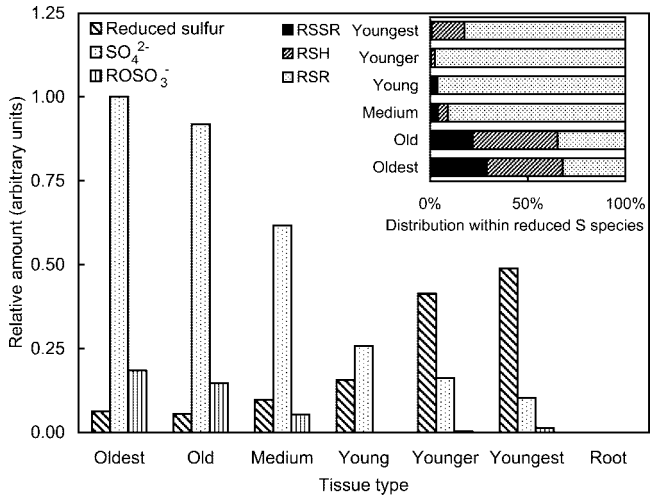

Figure 5. Relative amounts of S species in *A. bisulcatus* tissues. The amounts are arbitrarily normalized to the sulfate concentration in the oldest leaf sample, and are not on the same scale as those in Figure 3. The main figure shows the total reduced S (expressed as the sum of disulfides, thiols, and thioethers), whereas the inset shows the percentage distribution of these species.

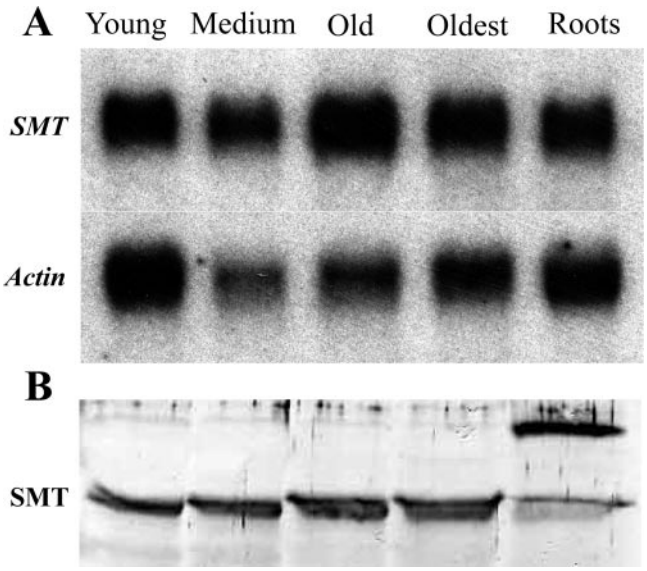

Figure 6. Northern- and western-blot analysis of seleno-Cys methyltransferase in *A. bisulcatus* tissues. A, Northern analysis of the steady-state levels of *SMT* mRNA in different *A. bisulcatus* tissues. After probing for *SMT*, the blots were stripped and reprobed with an Arabidopsis actin cDNA that acted as an internal loading control. B, Western analysis of SMT1 protein levels in different *A. bisulcatus* tissues. Each lane had 30 μg of total protein loaded.

and 7), and this reinforces the hypothesis that the accumulation of reduced forms does not depend upon seleno-Cys methyltransferase activity, but must be limited at an earlier stage in the pathway. Furthermore, the accumulation of selenate in the more mature leaves suggests that the initial two-electron reduction of selenate to selenite is limiting in these tissues.

The apparent decrease of selenate reduction capability of the older shoot tissue, as indicated by the predominance of selenate, is mirrored in the abundance of sulfate in these tissues (Fig. 5). This suggests that selenate and sulfate reduction are perhaps linked in *A. bisulcatus*. In the nonaccumulator plant Arabidopsis, ATP sulfurylase and APS reductase activity decline during aging of individual leaves (Rotte and Leustek, 2000). It is tempting to speculate that a similar decline in *A. bisulcatus* is responsible for the accumulation of sulfate in older leaf tissue. If S and Se biochemistry are closely linked, it would be reasonable to expect that a decline in the ability to reduce sulfate would be reflected in a decline in the ability to reduce selenate, as observed in old leaf tissue of *A. bisulcatus.* To better understand the linkage between sulfate and selenate reduction, it will be important to identify the enzymes responsible for these processes in *A. bisulcatus*.

The differential distribution of reduced and oxidized Se in young and old shoot tissue raises another interesting question. Our experiments did not track individual leaves as a function of time, but if mature leaves once had the Se distributions we observe in the young leaves, where did the Se-methylseleno-Cys go as they aged? We can speculate that Se-methylseleno-Cys may be metabolized, and the Se reoxidized to selenate as the leaves age, and then translocated within the plant. A more likely alternative is that the Se-methylseleno-Cys might be exported from the young shoot tissue as it ages, and accumulate in even younger tissues. For example, glutathione and *S*-methyl-Met are exported from leaves into the phloem (Rennenberg, 1982; Bourgis et al., 1999). The reduction in Se-methylseleno-Cys as the leaves age is not due to changes in leaf size; the young leaves that we used had attained fully grown size (i.e. young and old differed in size only by approximately 10%), and any slight changes in leaf size cannot explain the 40- to 60-fold decrease in the relative concentration of Se-methylseleno-Cys observed (Fig. 3) and quantified by Pickering et al. (2000). During the reproductive stage, it is likely exported to the seeds, which store extremely high levels of organic Se, and further work is needed to understand the mobility and distribution of Se in *A. bisulcatus*. It is also likely that the Se-methylseleno-Cys content of the leaf is reduced with increasing age by volatilization, predominantly as dimethyl diselenide (Evans et al., 1968), which is evidenced by the malodorous nature of the plants.

It seems very likely that the accumulation of Se by *A. bisulcatus* evolved as a defense against insect herbivores. Direct comparative data on insects is lacking, but by analogy with other animals (Ganther,

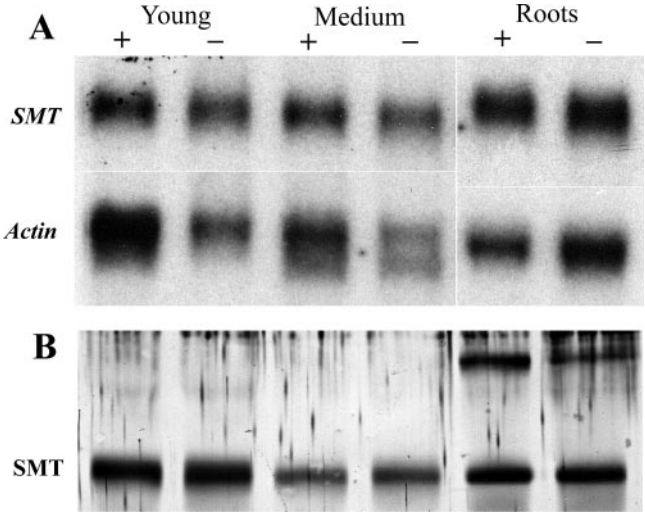

Figure 7. Northern- and western-blot analysis of seleno-Cys methyltransferase in *A. bisulcatus* exposed to selenate. A, Northern analysis of the steady-state levels of the *SMT1* mRNA in different *A. bisulcatus* tissues collected from plants that had been exposed to 5 μM selenate or untreated control plants. After probing with SMT1, the blots were stripped and reprobed with an Arabidopsis actin cDNA that acted as an internal loading control. B, Western analysis of SMT1 protein levels in different *A. bisulcatus* tissues collected from plants that had been exposed to 5 μM selenate or untreated control plants. Each lane had 30 μg of total protein loaded.

2001), selenate is likely to be much more toxic to insects than Se-methylseleno-Cys. Thus, the older leaves, despite the lower total Se content, are likely to be the most toxic. The young leaves, at growing shoot tips, may be more critical for plant survival than the older leaves, and we speculate that the volatile Se forms in the young leaves reduce their consumption by insects, which might be directed to nearby older leaves that contain potentially lethal levels of the more toxic selenate.

A complete understanding of the biochemistry of Se and S in *A. bisulcatus* will require more studies of the spatial dependence (Pickering et al., 2000) in addition to more in-depth biochemical studies. We have recently used microfocus techniques to image *A. bisulcatus* at cellular resolution (Pickering et al., 2002), and future work will address questions about the biochemistry and cellular location of the S and Se species in this unique plant.

MATERIALS AND METHODS

Plant Growth

Astragalus bisulcatus seeds were collected in August 1997 at Big Hollow, Wyoming by Catherine Skinner. To promote germination, seeds were vigorously shaken with concentrated sulfuric acid for 16 min, extensively washed with water, placed in a flask containing sterile water, and shaken at 150 rpm at 28°C for 2 h. Seeds were then allowed to germinate on filter paper moistened with deionized water for 5 d, and subsequently, approximately 10 seedlings were transferred into 12 L of hydroponic solution. Seedlings were initially supported by moist vermiculite, and later by cotton wool. Solutions were continuously aerated and exchanged weekly. The composition of all hydroponic solutions was as follows: 0.28 mM L^{-1} Ca^{2+}, 0.6 mM L^{-1} K^{+}, 0.2 mM L^{-1} Mg^{2+}, 0.025 mM L^{-1} NH_4^{+}, 1.16 mM L^{-1} NO_3^{-}, 0.025 mM L^{-1} $H_2PO_4^{-}$, 0.2 mM L^{-1} SO_4^{2-}, 4.75 μM L^{-1} ferric tartrate, 0.03 μM L^{-1} Cu^{2+}, 0.08 μM L^{-1} Zn^{2+}, 0.5 μM L^{-1} Mn^{2+}, 4.6 μM L^{-1} H_3BO_3, and 0.01 μM L^{-1} MoO_3, with 5 μM Se added as K_2SeO_4. Plants were cultivated in a growth chamber with a 12-h day period and day/night temperatures of 25°C/20°C. Fluorescent and incandescent lights provided 170 μmol m^{-2} s^{-1} of photosynthetic photon flux at the level of the plants. After 10 weeks of growth from the date of transfer into the hydroponic culture solution, some plants were separated into root and leaf tissues of different maturity (Fig. 1), divided into samples for Se x-ray absorption spectroscopy and northern and western analyses, rapidly frozen in liquid nitrogen, and stored at −80°C. Others were shipped live to the Stanford Synchrotron Radiation Laboratory (SSRL).

X-Ray Absorption Spectroscopy

Plant samples for Se K-edge x-ray absorption spectroscopy were shipped to SSRL on dry ice. To minimize breakdown and mixing of cellular components within the plant material, care was taken to keep the tissue frozen at all times before and during measurement. Frozen plant tissues were carefully ground under liquid nitrogen and were compacted into 2-mm path length Lucite sample holders with Mylar windows cooled in liquid nitrogen. During data collection, samples were held at approximately 15 K using a liquid helium cryostat. The short penetration depth of the beam at energies for S spectroscopy precluded the use of a liquid helium cryostat, and we used live tissue for these measurements. Plants were shipped to SSRL live in hydroponic solution, and measurements were carried out at room temperature on whole tissues to minimize tissue disruption. Whole leaf samples were arranged on adhesive Mylar tape to ensure complete coverage of the beam, and top and underside of the leaves were examined because the beam did not fully penetrate the samples. Samples were examined microscopically to check for radiation damage after exposure to the x-ray beam. No differences were observed until approximately 1 h after the 6-min exposure.

X-ray absorption spectroscopy data were collected at the SSRL using the program XAS Collect (George, 2000). Se K near-edge spectra were measured on beam line 7-3 using a Si(220) double-crystal monochromator, 1 mm upstream vertical aperture and no focusing optics. Harmonic rejection was achieved by detuning one monochromator crystal. Incident intensity was measured using a nitrogen-filled ion chamber, and the absorption spectrum was collected in fluorescence using a 13-element germanium detector. Spectra were energy calibrated with respect to a spectrum of hexagonal elemental Se, collected simultaneously with the spectrum of each sample, the first energy inflection of which is assumed to be 12,658.0 eV. Sulfur K near-edge x-ray absorption spectra were collected on beam line 6-2 essentially as previously described (Pickering et al., 1998) using a Si(111) monochromator and a downstream Ni-coated mirror. Incident intensity was measured using a He-filled ion chamber and the absorption spectrum using a Stern-Heald-Lytle fluorescence detector. The energy scale was calibrated with respect to the lowest energy peak of a sodium thiosulfate standard, which was assumed to be 2,469.2 eV (Sekiyama et al., 1986).

X-ray absorption spectroscopy data reduction was carried out using the EXAFSPAK suite of programs (http://ssrl.slac.stanford.edu/exafspak.html). Quantitative edge-fitting analysis was performed using the EXAFSPAK program DATFIT. Here, the near-edge spectrum of the plant material is fit, using a least-squares algorithm, to a linear combination of edge spectra from a library of Se or S model compounds (Pickering et al., 1995, 1998). The fractional contribution of each model spectrum to the fit is then equivalent to the fraction of S(e) present in that form in the plant material. Components were rejected if they contributed less than 1% or less than three times the estimated SD as determined from the fit. In the case of Se, the spectra were fit to spectra of aqueous selenate, selenite, and seleno-Met, but in all cases, the selenite was rejected. Seleno-Met is used as a surrogate for Se-methylseleno-Cys, whose spectrum is very similar (data not shown). In the case of S, the spectra used were oxidized glutathione, reduced glutathione, Met, methyl sulfate (shifted by 0.23 eV), and sulfate. Met sulfoxide (RS=OR) also contributed a very minor component in two cases. Spectra tested but excluded by the refinement included deprotonated Cys (RS^{-} measured experimentally at pH 13), Met sulfone, cysteic acid, and sulfite. Unless otherwise stated, all of the above standards were measured in buffered aqueous solution at close to neutral pH. Fit ranges were 12,600 to 12,750 eV for Se and 2,460 to 2,510 eV for S. However, in the S case, it was found that the sulfate species dominated for the mature leaves and so a second set of refinements was carried out in the restricted range 2,465 to 2,475 eV to better probe the organic S species.

The total amounts of S or Se species in the samples were determined by estimating the total edge jump. Relative amounts were then estimated by combining the total amounts with the fractional contributions. In the case of the S, the pair of spectra from the top and bottom of the leaves were found to give very similar results in each case, and so the values of relative amounts were averaged. Finally, relative amounts were normalized to sulfate (or selenate) in the oldest leaf sample. Note that the relative amount of Se and S thus obtained are on different arbitrary scales.

The accuracies of the estimations of the relative amounts are dependent on many factors, but errors derive principally from the edge-fitting analysis and from the estimation of quantities. The errors in determination of fractional makeup of species (using edge fitting) are estimated to be ±5% for the Se edge (Tokunaga et al., 1996), and are expected to be similar for S. For Se, the largest error in estimation of quantities likely depends on differences in sample packing and this may be as large as ±20%. For S, whole leaves were placed to ensure entire coverage of the beam and, in this case, quantities are expected to be much more accurate.

Cloning of Seleno-Cys Methyltransferase

The *A. bisulcatus SMT1* cDNA was amplified from shoot and root total RNA using RT-PCR. First strand cDNA was synthesized from total RNA using Avian Myeloblastosis Virus RT (Invitrogen, Carlsbad, CA). *SMT1* was amplified from first strand cDNA using TAQ polymerase with 5′-CAGGTACCATGTCGTCGCCATTGATAAC and 3′-GCTCTAGATGGTCACTTTGCAGAAAA as the 5′ and 3′ primers, respectively. Oligonucleotides used as primers were designed from the *SMT1* GenBank sequence (accession no. AJ131433). To allow directional cloning of the amplified *SMT1*

cDNA, the 5′ and 3′ primers were designed to contain KPN1 and *Xba*I restriction enzyme sites, respectively. PCR amplification gave rise to a single major cDNA species with the expected size of approximately 1 Kb. This 1-Kb fragment was partially purified from the RT-PCR reaction mixture using phenol/chloroform extraction, ammonium acetate/isopropanol precipitation (−80°C), ethanol washing, and resuspension in water. For cloning of the *SMT1* cDNA, partially purified cDNA and pZErO-2 (Invitrogen) were combined and digested with *Xba*I and KPN1 for 10 min at 37°C. Digested products were partially purified using phenol/chloroform extraction, ammonium acetate/isopropanol precipitation (−80°C), ethanol washing, and resuspension in water. The partially purified cDNA pZErO-2 mixture was ligated using DNA ligase, and the reaction was allowed to proceed at 4°C for 1 h. Chemically competent *Escherichia coli* cells (strain TOP10 F^-) were transformed with the ligation mixture, and were transformants selected on Luria-Bertani broth plates containing kanamycin (50 μg mL^{-1}). Plasmids were isolated from randomly picked transformed colonies, and cDNA insert size was determined by restriction digestion (*Xba*I and KPN1) and 1.5% (w/v) agarose gel electrophoresis. Clones that contained a cDNA of approximately 1 Kb were selected and identified by sequencing at the University of Arizona sequencing facility.

RNA-Blot Analysis

Total RNA was isolated according to Puissant and Houdebine (1990), and the northern blot was prepared and probed following previously described protocols (Persans et al., 1999) with the following exceptions: cDNA probes were prepared by digesting pZErO-2 containing the *SMT1* with *Xba*I and KPN1, and pZL-1 containing an Arabidopsis actin gene (GenBank accession no. U37281) with *Bam*HI and *Eco*RI for 1 h at 37°C. The resulting fragments were run on a 1.5% (w/v) agarose gel, and the appropriate size fragment was excised from the gel and recovered by electroelution. For *SMT1*, the resulting fragment was approximately 1 Kb in size, and contained only protein coding sequence.

Immunoblot Analysis

SDS-PAGE was performed according to Laemmli (1970). Crude extracts of *A. bisulcatus* were obtained by grinding tissue samples in liquid nitrogen and mixing the frozen powdered plant material in a 1:1 ratio (w/v) with SDS sample buffer. The mixture was boiled for 10 to 15 min and was centrifuged at 16,000*g*. The supernatant was assayed for total protein concentration using bicinchoninic acid (Pierce, Rockford, IL) and equal amounts of protein loaded on an SDS-PAGE gel. For immunoblotting, proteins were transferred from the SDS-PAGE gel onto an Immuno-Blot polyvinylidene difluoride membrane (Bio-Rad, Hercules CA) using electrophoretic semidry blotting. Seleno-Cys methyltransferase was visualized on the membrane using a polyclonal primary antibody raised against SMT in rabbits (Neuhierl et al., 1999), and a secondary anti-immunoglobulin G antibody raised in goat and conjugated to alkaline phosphatase. Blots were developed by the addition of nitroblue tetrazolium/5-bromo-4-chloro-3-indolylphosphate.

ACKNOWLEDGMENTS

We thank Dr. August Böck for kindly providing the anti-seleno-Cys methyltransferase antibodies and Lin Huyah for preparation of Figure 1.

Received September 17, 2002; returned for revision November 8, 2002; accepted November 29, 2002.

LITERATURE CITED

Barak P, Goldman IL (1997) Antagonistic relationship between selenate and sulfate uptake in Onion (*Allium cepa*): implications for the production of organosulfur and organoselenium compounds in plants. J Agric Food Chem **45:** 1290–1294

Bourgis F, Roje S, Nuccio ML, Fisher DB, Tarczynski MC, Li C, Herschbach C, Rennenberg H, Pimenta MJ, Shen T-L et al. (1999) *S*-Methylmethionine plays a major role in phloem sulfur transport and is synthesized by a novel type of methyltransferase. Plant Cell **11:** 1485–1497

Brown TA, Shrift A (1982) Selenium: toxicity and tolerance in higher plants. Biol Rev **57:** 59–84

Burnell JN (1981) Selenium metabolism in *Neptunia amplexicaulis*. Plant Physiol **67:** 316–324

Byers HG (1936) Selenium occurrence in certain soils in the United States, with a discussion of related topics. Second report. U.S. Dept Agric Technol Bull **530**

Clark LC, Combs GF Jr, Turnbull BW, Slate EH, Chalker DK, Chow J, Davis LS, Glover RA, Graham GF, Gross EG et al. (1996) Effects of selenium supplementation for cancer prevention in patients with carcinoma of the skin: a randomized controlled trial. Nutritional Prevention of Cancer Study Group. J Am Med Assoc **276:** 1957–1963

Combs GF Jr, Clark LC, Turnbull BW (1997) Reduction of cancer risk with oral supplement of selenium. Biomed Environ Sci **10:** 227–234

de Souza MP, Pilon-Smits EA, Lytle CM, Hwang S, Tai J, Honma TS, Yeh L, Terry N (1998) Rate-limiting steps in selenium assimilation and volatilization by Indian mustard. Plant Physiol **117:** 1487–1494

Dilworth GL, Bandurski RS (1977) Activation of selenate by adenosine 5′-triphosphate sulphurylase from *Saccharomyces cerevisiae*. Biochem J **163:** 521–529

Evans CS, Asher CJ, Johnson CM (1968) Isolation of dimethyl diselenide and other volatile selenium compounds from *Astragalus racemosus* (Pursh.). Aust J Bio Sci **21:** 13–20

Ganther HE (2001) Selenium metabolism and mechanisms of cancer prevention. Adv Exp Med Biol **492:** 119–130

Ip C, Lisk DJ, Scimeca JA (1994) Potential of food modification in cancer prevention. Cancer Res **54:** 1957s–1959s

Laemmli UK (1970) Cleavage of structural proteins during the assembly of the head of bacteriophage T4. Nature **277:** 680–685

George MJ (2000) XAS-Collect: a computer program for X-ray absorption spectroscopic data acquisition. J Synchrotron Rad **7:** 283–286

McCluskey TJ, Scarf AR, Anderson JW (1986) Enzyme catalyzed $\alpha\beta$-elimination of selenocystathionine and selenocystine and their sulphur isologues by plant extracts. Phytochemistry **25:** 2063–2068

Mikkelsen RL, Wan HF (1990) The effect of selenium on sulfur uptake by barley and rice. Plant Soil **121:** 151–153

Muller S, Heider J, Bock A (1997) The path of unspecific incorporation of selenium in *Escherichia coli*. Arch Microbiol **168:** 421–427

Neuhierl B, Böck A (1996) On the mechanism of selenium tolerance in selenium-accumulating plants: purification and characterization of a specific selenocysteine methyltransferase from cultured cells of *Astragalus bisulcatus*. Eur J Biochem **239:** 235–238

Neuhierl B, Thanbichler M, Lottspeich F, Böck A (1999) A family of *S*-methylmethionine-dependent thiol/selenol methyltransferases: role in selenium tolerance and evolutionary relation. J Biol Chem **274:** 5407–5414

Ng BH, Anderson JW (1978) Synthesis of selenocysteine by cysteine synthase from selenium accumulator and non-accumulator plants. Phytochemistry **17:** 2069–2074

Orser CS, Salt DE, Pickering IJ, Prince R, Epstein A, Ensley BD (1999) Brassica plants to provide enhanced human mineral nutrition: selenium phytoenrichment and metabolic transformation. J Med Food **1:** 253–261

Persans M, Xiange Y, Patnoe JMML, Krämer U, Salt DE (1999) Molecular dissection of histidine's role in nickel hyperaccumulation in *Thlaspi goesingense* (Hálácsy). Plant Physiol **121:** 1–10

Petersen BL, Chen S, Hansen CH, Olsen CE, Halkier BA (2002) Composition and content of glucosinolates in developing *Arabidopsis thaliana*. Planta **214:** 562–571

Pickering IJ, Brown GE Jr, Tokunaga TK (1995) Quantitative speciation of selenium in soils using X-ray absorption spectroscopy. Environ Sci Technol **29:** 2456–2459

Pickering IJ, George GN, Van Fleet-Stalder V, Chasteen TG, Prince RC (1999) X-ray absorption spectroscopy of selenium-containing amino acids. J Biol Inorg Chem **4:** 791–794

Pickering IJ, Hirsch G, Prince RC, Yu EY, Salt DE, George GN (2002) Imaging of selenium in plants using tapered metal monocapillary optics. J Synchrotron Rad (submitted)

Pickering IJ, Prince RC, Divers T, George GN (1998) Sulfur K-edge X-ray absorption spectroscopy for determining the chemical speciation of sulfur in biological systems. FEBS Lett **441:** 11–14

Pickering IJ, Prince RC, Salt DE, George GN (2000) Quantitative chemically-specific imaging of selenium transformation in plants. Proc Natl Acad Sci USA **97:** 10717–10722

Pilon-Smits EAH, Hwang S, Lytle CM, Zhu Y, Tai JC, Bravo RC, Chen Y, Leustek T, Terry N (1999) Overexpression of ATP sulfurylase in Indian

mustard leads to increased selenate uptake, reduction, and tolerance. Plant Physiol **119:** 123–132

Puissant C, Houdebine LM (1990) An improvement of the single-step method of RNA isolation by acid guanidinium thiocyanate-phenol-chloroform extraction. BioTechniques **8:** 148–149

Rennenberg H (1982) Glutathione metabolism and possible biological roles in higher plants. Phytochemistry **1:** 2771–2781

Rotte C, Leustek T (2000) Differential subcellular localization and expression of ATP sulfurylase and 5′-adenylylsulfate reductase during ontogenesis of Arabidopsis leaves indicates that cytosolic and plastid forms of ATP sulfurylase may have specialized functions. Plant Physiol **124:** 715–724

Sabaty M, Avazeri C, Pignol D, Vermeglio A (2001) Characterization of the reduction of selenate and tellurite by nitrate reductases. Appl Environ Microbiol **143:** 1181–1189

Salt DE, Smith RD, Raskin I (1998) Phytoremediation. Annu Rev Plant Physiol Plant Mol Biol **49:** 643–668

Schafer FQ, Buettner GR (2001) Redox environment of the cell as viewed through the redox state of the glutathione disulfide/glutathione couple. Free Radical Biol Med **30:** 1191–1212

Sekiyama H, Kosugi N, Kuroda H, Ohta T (1986) Sulfur K-edge absorption spectra of Na_2SO_4, Na_2SO_3, $Na_2S_2O_3$, and $Na_2S_2O_x$ ($x = 5 - 8$). Bull Chem Soc Jpn **59:** 575–579

Setya A, Murillo M, Leustek T (1996) Sulfate reduction in higher plants: molecular evidence for a novel 5′-adenylylsulfate reductase. Proc Natl Acad Sci USA **93:** 13383–13388

Shaw WH, Anderson JW (1972) Purification, properties and substrate specificity of adenosine triphosphate sulfurylase from spinach leaf tissue. Biochem J **127:** 237–247

Shaw WH, Anderson JW (1974) Comparative enzymology of the adenosine triphosphate sulphurylase from leaf tissue of selenium-accumulator and non-accumulator plants. Biochem J **139:** 37–42

Shrift A (1969) Aspects of selenium metabolism in higher plants. Annu Rev Plant Physiol **20:** 475–495

Shrift A, Virupaksha TK (1965) Seleno-amino acids in selenium-accumulating plants. Biochim Biophys Acta **100:** 65–75

Tokunaga TK, Pickering IJ, Brown GE Jr (1996) Selenium transformations in ponded sediments. Soil Sci Soc Am J **60:** 781–790

Trelease SF, Di Somma AA, Jacobs AL (1960) Seleno-amino acid found in *Astragalus bisulcatus*. Science **132:** 618

Virupaksha TK, Shrift A (1965) Biochemical differences between selenium accumulator and non-accumulator *Astragalus* species. Biochim Biophys Acta **107:** 69–80

Wang Y, Bock A, Neuhierl B (1999) Acquisition of selenium tolerance by a selenium non-accumulating *Astragalus* species via selection. Biofactors **9:** 3–10

Williams MJ, Ogle RS, Knight AW, Burau RG (1994) Effects of sulfate on selenate uptake and toxicity in the green alga *Selenastrum capricornutum*. Arch Environ Contam Toxicol **27:** 449–453

Yu EY, Pickering IJ, George GN, Prince RC (2001) In situ observation of the generation of isothiocyanates from sinigrin in horseradish and wasabi. Biochim Biophys Acta **1527:** 156–160